# Cooperative Spectrum Prediction for Improved Efficiency of Cognitive Radio Networks

by

**Nagwa Shaghluf**

B.S., Tripoli University, Tripoli, Libya, 2009

A Thesis Submitted in Partial Fulfillment
of the Requirements for the Degree of

**MASTER OF APPLIED SCIENCE**

in the Department of Electrical & Computer Engineering

# Cooperative Spectrum Prediction for Improved Efficiency of Cognitive Radio Networks

by

**Nagwa Shaghluf**

## Supervisory Committee

---

Dr. T. Aaron Gulliver, (Department of Electrical & Computer Engineering)
**Supervisor**

---

Dr. Xiaodai Dong, (Department of Electrical & Computer Engineering)
**Departmental Member**

# Abstract

In this thesis, the spectrum and energy efficiency of cooperative spectrum prediction (CSP) in cognitive radio networks are investigated. In addition, the performance of CSP is evaluated using a hidden Markov model (HMM) and a multilayer perceptron (MLP) neural network. The cooperation between secondary users in predicting the next channel status employs AND, OR and majority rule fusion schemes. These schemes are compared for HMM and MLP predictors as a function of channel occupancy in terms of prediction error, spectrum efficiency and energy efficiency. The impact of busy and idle state prediction errors on the spectrum efficiency is determined. Further, the spectrum efficiency is compared for different numbers of primary users (PUs).

Simulation results are presented which show a significant improvement in the spectrum efficiency using CSP with the majority rule at the cost of a small degradation in energy efficiency compared to single spectrum prediction (SSP) and traditional spectrum sensing (TSS). The HMM predictor provides better performance than the MLP predictor. Moreover, the total probability of prediction error with the majority rule provides the best performance compared to SSP and the other fusion rules. On the other hand, the AND and OR rules have the worst performance in the high and low traffic cases, respectively. The majority rule provides a good tradeoff between busy and idle state prediction errors compared with the AND and OR rules and SSP. Further, a reduction in the busy state prediction error increases the SE more compared to a reduction in the idle state prediction error.

# Table of Contents

# List of Tables

# List of Figures

# Acknowledgments

All praise and thanks is due to Allah, for giving me the capability to complete this thesis.

I would like to extend my gratitude to my supervisor, Dr. T. Aaron Gulliver, for his support, advice, and guidance throughout my research. I would also like to extend my appreciation and gratitude to Dr. Xiaodai Dong for serving on my supervisory committee.

I would also like to acknowledge the Libyan Ministry of Higher Education and Scientific Research for supporting me financially.

# Dedication

I would like to dedicate this thesis to the memory of my father, who was my greatest supporter, to my beloved husband, for his love and support, to my wonderful daughters Yasmine and Ayat, for giving me the smile that I needed every day, and to my mother, sister and brothers for giving me the encouragement and strength I needed to complete my goals.

# List of Acronyms

| | |
|---|---|
| AWGN | Additive white Gaussian noise |
| CR | Cognitive radio |
| CRN | Cognitive radio network |
| CSS | Cooperative spectrum sensing |
| FC | Fusion center |
| SNR | Signal to noise ratio |
| TSS | Traditional spectrum sensing |
| SSP | Single spectrum prediction |
| CSP | Cooperative spectrum prediction |
| HMM | Hidden Markov model |
| NN | Neural network |
| BWA | The Baum-Welch algorithm |
| VA | Viterbi algorithm |
| DSA | Dynamic spectrum allocation |
| ED | Energy detector |
| FCC | Federal Communications Commission |
| FSA | Fixed spectrum allocation |
| MLP | Multilayer perceptron |
| ANN | Artificial neural network |
| BP | Backpropagation |
| PU | Primary user |
| SE | Spectrum efficiency |
| EE | Energy efficiency |
| SS | Spectrum sensing |
| SU | Secondary user |

# List of Symbols

| | |
|---|---|
| $P_f$ | Probability of false alarm |
| $P_m$ | Probability of misdetection |
| $P_d$ | Probability of detection |
| $v(t)$ | Received signal at the SU |
| $g(t)$ | Transmitted PU signal |
| $h$ | Channel gain |
| $n(t)$ | Zero-mean AWGN |
| $H_1$ | Binary hypothesis of PU presence |
| $H_0$ | Binary hypothesis of PU absence |
| $W$ | Bandwidth of the ED bandpass filter |
| $\tau_s$ | Sensing period |
| $Y$ | Output of the ED integrator |
| $\zeta$ | ED threshold |
| $Decision_{ED}$ | ED decision result |
| $Decision$ | SS decision result |
| $S$ | PU occupancy state |
| $L$ | Length of the observation sequence |
| $O$ | Observation sequence |
| $O_l$ | Observation state at time $l$ |
| $S_l$ | Hidden state at time $l$ |
| $\lambda\ (\pi, A, B)$ | HMM parameters |

| | |
|---|---|
| $\pi$ | Initial state distribution |
| $A$ | Transitions probability matrix |
| $B$ | Emission matrix |
| $\beta_l(i)$ | HMM backward variable |
| $\xi_l(i,j)$ | Probability of being in state $i$ at time $l$ and in state $j$ at time $l+1$ |
| $\gamma_l(i,j)$ | Probability of being in state $i$ at time $l$ given $O$ |
| $\widehat{a_{ij}}$ | Re-estimation of $a_{ij}$ |
| $\widehat{b_{jk}}$ | Re-estimation of $b_{jk}$ |
| $\widehat{\pi_i}$ | Re-estimation of $\pi_i$ |
| $D_{L+1}$ | HMM prediction decision |
| $x_{L+1}$ | Predicted state of the MLP predictor at state $L+1$ |
| $r$ | Number of hidden layers in the MLP predictor |
| $y_j^r$ | Output of neuron $j$ at the $r$th layer of the MLP predictor |
| $v_j^r$ | Weighted sum of the inputs |
| $w_{ji}^r$ | Adaptive weight |
| $\widehat{x_{L+1}}$ | Desired output of the MLP predictor |
| $G_{L+1}$ | MLP prediction decision |
| $e_L$ | Error at the MLP output |
| $E$ | Mean square error of the MLP predictor |
| $P_p^e(\text{Total})$ | Total probability of an SSP prediction error |
| $P_p^e(\text{Busy})$ | Probability of an SSP prediction error for a busy channel state |
| $P_p^e(\text{Idle})$ | Probability of an SSP prediction error for an idle channel state |

| | |
|---|---|
| $\overline{P_p^e(\text{Total})}$ | Total probability of a CSP prediction error |
| $\overline{P_p^e(\text{Busy})}$ | Probability of a CSP prediction error for a busy channel state |
| $\overline{P_p^e(\text{Idle})}$ | Probability of a CSP prediction error for an idle channel state |
| $F$ | Global prediction decision at the FC |
| $Z$ | FC rule decision threshold |
| $M$ | Number of SUs |
| $N$ | Number of PUs |
| μ | Probability of remaining in the idle state |
| $\theta$ | Probability of remaining in the busy state |
| $P_i$ | Probability of an idle PU channel |
| $P_b$ | Probability of a busy PU channel |
| $T$ | SU frame period |
| $\tau_p$ | Prediction period |
| $\tau_s$ | Sensing period |
| $\tau_t$ | Transmission period |
| $\tau_r$ | Reporting time |
| $C_0$ | SE in the absence of a PU |
| $C_1$ | SE in the present of the PU |
| $SNR_s$ | SNR of the SU at the SU receiver |
| $SNR_p$ | SNR of the PU at the SU receiver |
| $P_p^0$ | Probability of predicting an idle state for a PU channel |
| $P_p^1$ | Probability of predicting a busy state for a PU channel |
| $P_N^0$ | Probability of predicting at least one PU channel at an idle state |

| | |
|---|---|
| $P_N^1$ | Probability of predicting that every PU channel is in the busy state |
| $C_N^k$ | Binomial coefficient for $k$ elements from a set of $N$ elements |
| $SE_{avg}$ | Average SE |
| $SE_{norm}$ | Normalized SE |
| $SE_{upper}$ | SE upper bound |
| $P_p$ | Prediction power |
| $P_r$ | Reporting power |
| $P_s$ | Sensing power |
| $P_T$ | Transmission power |
| $E_{avg-CSP}$ | Average CSP energy consumption |
| $E_{avg-TSS}$ | Average TSS energy consumption |
| $E_{avg-SSP}$ | Average SSP energy consumption |

# Chapter 1

## Introduction

The rapid growth of services and applications in wireless communication networks has created a huge need for additional frequency spectrum. It is hard to satisfy this need with the limited spectrum resources and fixed spectrum allocation (FSA). In FSA, licensed users are assigned to operate only in specific frequency bands and they may not efficiently utilize these bands as shown in Figure 1.1.

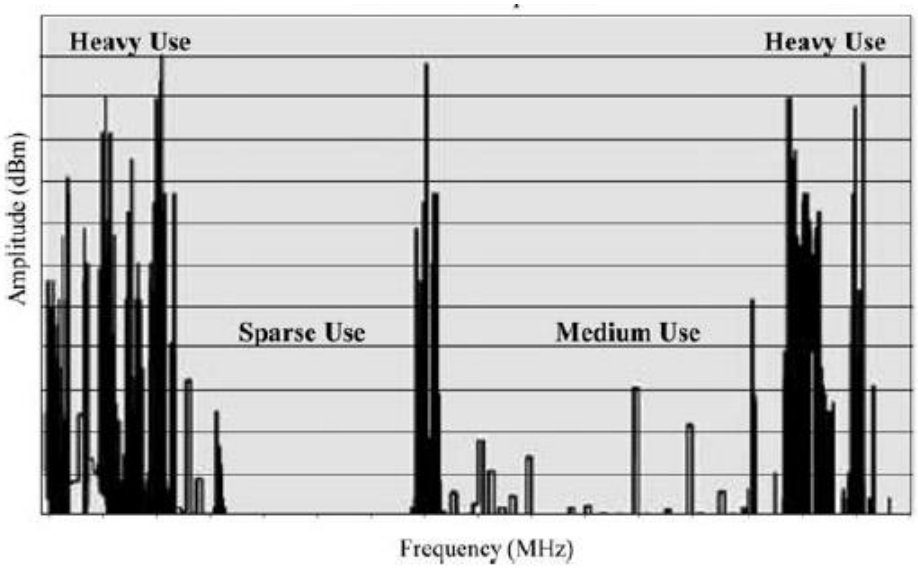


**Figure 1.1:** Spectrum utilization [2].

The spectrum allocation is managed by government organizations such as the Federal Communications Commission (FCC). The FCC has reported that large portions of spectrum are highly underutilized, and the temporal and geographic variations in spectrum utilization range from 15% to 85% [2]. This inefficiency has created the need for a new spectrum management paradigm. Thus, dynamic spectrum allocation (DSA) has been proposed. DSA allows unlicensed users to opportunistically utilize the unused spectrum of the licensed users. In DSA, the absence of a licensed user is referred to as a spectrum opportunity, a spectrum hall, or a white space as shown in Figure 1.2. In this thesis, this is called a spectrum opportunity.

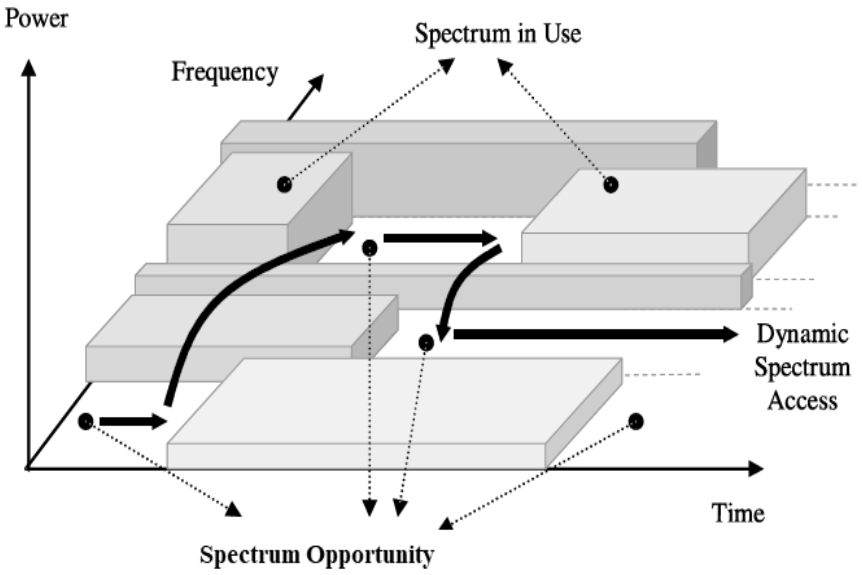


**Figure 1.2:** Dynamic spectrum access [2].

## 1.1 Overview of Cognitive Radio Networks

Cognitive radio networks (CRNs) are seen as future wireless communication networks which allow DSA for the licensed spectrum [1]. In a CRN, the licensed spectrum

consists of a number of licensed channels defined by specific bandwidths. Licensed users have priority in accessing these channels. Unlicensed user can opportunistically access licensed channels in the absence of licensed users. Thus, licensed users are referred to as primary users (PUs) and unlicensed users are referred to as secondary users (SUs) [2]. The main component of the CRN is the cognitive radio (CR) transceiver, which is an enabling technology for DSA. CR was first defined by Mitola in 1999 based on a software-defined radio platform [3]. A CR is an intelligent wireless communication system that has two characteristics, cognitive capability and reconfigurability. Cognitive capability refers to the ability to obtain information about the surrounding radio environment by sensing and capturing temporal and spatial variations. Reconfigurability refers to the ability to change transmission power, operating frequency and bandwidth according to specific PU communication parameters [2].

A CRN can be classified as a centralized network or a distributed network [4]. In a centralized CRN, a central node acts as a controlling node to manage the communications between SUs. In a distributed CRN, an SU is able to communicate directly with other SUs in its transmission range, and one SU is chosen as a head node [4]. In this thesis, a centralized CRN is considered. The main CRN functions are as follows [2].

1. Spectrum sensing (SS): the ability of an SU to detect a spectrum opportunity. The main focus of this thesis is SS.
2. Spectrum management: the ability to choose the best spectrum for SU use.
3. Spectrum mobility: the ability to find new available spectrum with minimum delay when the PU appears in the current spectrum.

4. Spectrum sharing: the ability of a CRN to share the available spectrum among the SUs.

## 1.2 Motivation

CRN performance is significantly affected by the SS. Inaccurate decisions about spectrum opportunities results in increased PU interference, increased delay, and spectrum efficiency (SE) degradation. Further, selecting channels randomly to perform SS in a high traffic CRN results in long wait times and high energy consumption, which degrades the SE and energy efficiency (EE) of the network. For this reason, spectrum occupancy prediction has been proposed to predict PU channel occupancy based on historical sensing information [8]. In this case, SUs only have to sense channels that are predicted to be idle in the next time slot. This results in increased SE, efficient channel selection, and reduced power consumption due to sensing busy channels. To improve the prediction performance, cooperative spectrum prediction (CSP) has been proposed in [9, 10, 11], which is a cooperative approach to obtain a prediction decision about the spectrum. Recently, increasing the SE and EE has attracted much attention as it can improve CRN performance and reduce the required power. However, increasing the SE can decrease the EE [5]. Thus, this thesis investigates the performance of a CRN with CSP in terms of the SE and EE.

## 1.3 Contributions

The main contributions of this thesis are three fold. First, the prediction performance of CSP as a function of PU channel occupancy is investigated. This is done in terms of the total probability of prediction error and the probability of prediction error for busy and idle channel status, which is employed using AND, OR and majority rule fusion schemes.

Further, the prediction performance of CSP is compared to traditional spectrum sensing (TSS) and single spectrum prediction (SSP). Second, the CRN performance with CSP is investigated. This is done in term of the SE and EE. Further, the effect of the probability of prediction error on the SE for busy and idle channel status is investigated. Third, SE performance with CSP is evaluated for different numbers of PU channels.

## 1.4 Thesis Outline

In this chapter, an introduction to DSA and CRNs was provided. Further, the motivation and contributions of this thesis were presented. **Chapter 2** reviews spectrum occupancy prediction and its performance evaluation starting with an introduction to SS and cooperative spectrum sensing (CSS). Further, energy detection and the performance evaluation of SS are described. In addition, HMM and MLP predictors are described in detail, and centralized and decentralized CSP are introduced. Finally, pre-fusion CSP and post-fusion CSP are illustrated. Furthermore, the types of data fusion are presented. **Chapter 3** studies CRN performance with CSP, reviews the related research, and describes the proposed system model for CSP which is based on pre-fusion CSP in a centralized CRN. Further, the performance evaluation of CSP is presented in terms of the probability of prediction error, SE and EE, using an analytical evaluation for the SE and EE. **Chapter 4** presents the performance evaluation of the proposed model. Simulation results for HMM and MLP predictors are presented for CSP and SSP in terms of probability of prediction error. In addition, numerical results for SE and EE with CSP are presented and compared with the results for TSS and SSP. This is done using the simulation results for the HMM and MLP predictors and for different numbers of PU channels. **Chapter 5** concludes the thesis and provides directions for future research.

# Chapter 2

# Background

In reactive DSA, an SU first senses the spectrum and then reacts by initiating transmission when the PU is sensed to be idle. However, the PU can appear at any time and the SU must immediately vacate the spectrum and sense another channel [12]. Thus, reactive DSA can result in large delays, interference to the PU and disturbance to SU transmission. Moreover, in high traffic CRNs, random PU channel selection to perform SS can result in missed spectrum opportunities and large delays which degrades the CRN performance. Therefore, proactive DSA has been proposed which allows PU spectrum occupancy prediction. In proactive DSA, an SU selects channels based on availability, potential transmission time and quality of service. This results in less SU disturbance, less delay in searching for an idle PU channel and less PU interference compared to reactive DSA. Cooperation among SUs has been exploited in [9, 10, 11] to enhance the spectrum prediction performance compared to SSP.

## 2.1 Spectrum Sensing

SS is one of the major functions of CRNs as it affects other CRN functions such as spectrum decisions, spectrum sharing, and spectrum mobility. Further, SS affects CRN performance such as spectrum efficiency (SE) and energy efficiency (EE). SE is the ability of an SU to efficiently utilize the unused PU spectrum, while EE is defined as the ratio of

SE to the total power consumed by the SU [5]. EE is an important factor especially for battery-powered devices and environmental concerns.

The local sensing observation of an SU can be formulated as a binary hypothesis problem

$$v(t) = \begin{cases} n(t), & H_0 \\ h\,g(t) + n(t), & H_1 \end{cases} \tag{2.1}$$

where $v(t)$ is the received signal at the SU, $g(t)$ is the PU signal, $h$ is the channel gain and $n(t)$ is zero-mean additive white Gaussian noise (AWGN). $H_1$ and $H_0$ are the binary hypotheses which define the presence and absence of the PU, respectively [2].

SS detection techniques can be classified as coherent or non-coherent [6]. With coherent detection, prior knowledge of the PU signal characteristics is required. In non-coherent detection, no prior knowledge is required for PU detection. Energy detection (ED) is a non-coherent detection technique [6] and is used in this thesis.

ED is one of the most common PU detection techniques as it has low computational and implementation complexities and requires no prior information about the PU [7]. An ED block diagram is shown in Figure 2.1. To measure the energy of the received signal $Y$, the output of the bandpass filter of width $W$ is squared and then integrated over the sensing period $\tau_s$. Finally, $Y$ is compared with the threshold $\zeta$ [2]. The ED decision is

$$Decision_{ED} = \begin{cases} H_0, & Y < \zeta \\ H_1, & Y \geq \zeta \end{cases} \tag{2.2}$$

One of the disadvantages of ED is the poor performance when the PU signal is weak, which can result in a wrong sensing decision.

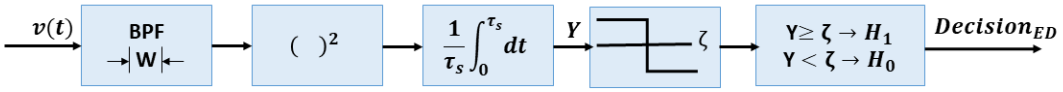


**Figure 2.1:** Energy detection based sensing block diagram.

SS techniques are classified as non-cooperative SS or cooperative spectrum sensing (CSS). In non-cooperative SS, the sensing observation is done independently by a single SU. In this thesis, a non-cooperative SS is referred to traditional spectrum sensing (TSS). In CSS, a number of SUs cooperate and share their sensing observations to obtain a reliable decision.

CSS has been proposed as a solution to enhance the detection performance of SS. This is done by taking advantage of the spatial diversity of SUs in a CRN to mitigate the effects of multi path fading and shadowing. The detection performance improvement with CSS is referred to as cooperative gain. Further, the cooperative overhead is the extra sensing time, sensing energy, delay and computational complexity created by using CSS. CSS is ineffective when the SUs are affected by the same shadowing and multi path fading. Consequently, the cooperative gain of CSS is affected by SU selection, and increasing the area for cooperative SU can increase the cooperative gain [6].

## 2.2 Spectrum Sensing Performance

Local SS performance is determined by the probability of false alarm ($P_f$) and the probability of misdetection ($P_m$). $P_f$ is the probability of wrongly sensing an idle PU

channel and $P_m$ is the probability of wrongly sensing a busy PU channel [6].

$$P_m = \{Decision = H_0 | H_1\} \quad (2.3)$$

$$P_f = \{Decision = H_1 | H_0\} \quad (2.4)$$

where $Decision$ is the decision result of SS technique. For reliable SS performance, a detection performance with lower $P_m$ and $P_f$ is required, to improve the throughput and avoid PU interference. Therefore, $P_m$ and $P_f$ are defined as [2, 6, 7]. The probability of detection ($P_d$) is the probability of correctly sensing a busy PU channel and is given by

$$P_d = 1 - P_m = \{Decision = H_1 | H_1\} \quad (2.5)$$

## 2.3 Spectrum Occupancy Prediction

In CRNs, an SU can predict the future state of PU channel by learning from past sensing results or modeling the PU channel occupancy [7]. Modeling PU channel occupancy is very important for CRNs as it can reduce the SU disturbance rate and PU interference [12]. In prediction-based learning, the state of a PU channel (idle or busy) is predicted based on past SS results for that channel. Consequently, spectrum occupancy prediction can decrease the sensing time and energy for a busy channel, decrease the SU disturbance rate and lower the PU interference.

Spectrum occupancy prediction can be used for the CRN functions. In prediction-based spectrum sensing, an SU can skip SS for channels that are predicted to be idle. In prediction-based spectrum decisions, an SU can select a high-quality PU channel (high idle probability, large idle duration) for SS and accessing. In prediction-based spectrum

mobility, an SU can predict the appearance of a PU and vacate the spectrum before this occurs [8]. In this thesis, a prediction-based spectrum sensing is considered.

Spectrum occupancy prediction is classified as either SSP or CSP. In SSP, the prediction is done locally by a single SU. In CSP, the prediction is done by a group of SUs [9, 10, 11]. The spectrum occupancy prediction can be classified into two categories. The first category assumes a traffic model for the PUs and prediction is carried out using this model. Several PU traffic models have been proposed for CRNs [12]. PU traffic models have been proposed which are based on Markov processes, queuing theory, ON/OFF periods and time series. Some of the disadvantages of these models are high computational complexity, poor fit with real data and an inability to capture small variations in channel occupancy [12]. The second category models the PU channel occupancy by learning from past SS results. In this thesis, the focus is on the most widely used learning techniques, namely a two state HMM and an artificial neural network (ANN).

### 2.3.1 Spectrum Occupancy Modeling Using HMM

In HMM based prediction, the system is considered as a Markov process of hidden states which are evaluated using a set of observation states [12], as shown in Figure 2.2. The observation sequence is the last $L$ sensing time slots so that $\boldsymbol{O} = (O_1, O_2, \ldots, O_L) \in \{0,1\}$. $L$ should be large enough to accurately train the HMM. The objective of the HMM is to predict the state $O_{L+1}$. $O_l$ and $S_l$ are the observation state and hidden state, respectively, at time $l$, where $1 \leq l \leq L$. For a CRN, the PU true channel state $S$ (idle or busy) is considered by the HMM to be hidden from the observer (SU), and the observation states are the historical sensing information. In two state HMM-based spectrum prediction, $S \in \{0, 1\}$ where 0 denotes an idle channel state and 1denotes a busy channel state.

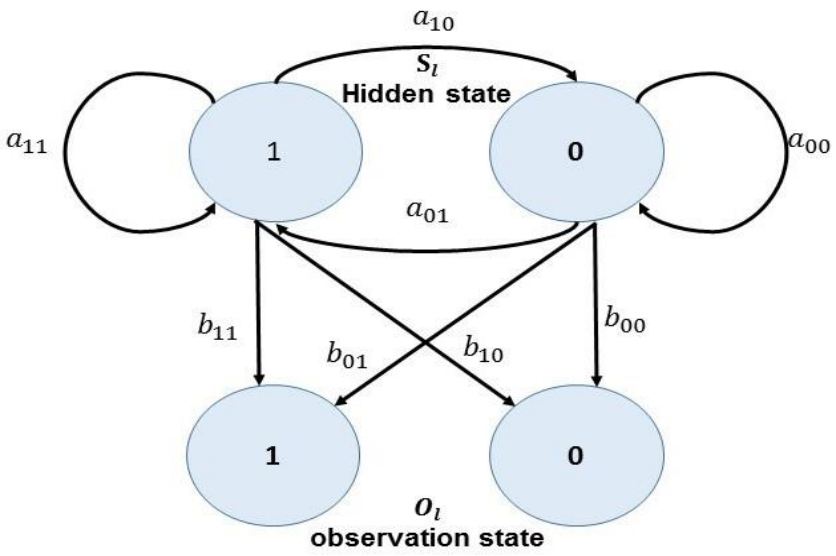


**Figure 2.2:** Two state hidden Markov model.

The HMM is defined by $\lambda\,(\pi, A, B)$ [13, 14, 15], where $\pi$ is the initial state distribution, $A$ is the transitions probability matrix and $B$ is the emission matrix. $\pi, A$ and $B$ are defined as $\pi = [\pi_i]_{1\times 2}, \quad \pi_i \leq 1,\ \sum_{i=0}^{1}\pi_i = 1, \quad A = \left[a_{ij}\right]_{2\times 2},\ a_{ij} = P(S_{l+1} = j|S_l = i),\ i,j \in O$ and $B = \left[b_{jk}\right]_{2\times 2},\ b_{jk} = P(O_l = k|S_l = j),\ k \in S,\ j \in O$. Thus, $b_{11} = P_d$ and $b_{01} = P_f$. The HMM predictor model is shown in Figure 2.3. To predict $O_{L+1}$, $\lambda\,(\pi, A, B)$ should generate the same observation sequence with maximum likelihood probability $P(O|\lambda)$. $P(O_L, 0|\lambda)$ and $P(O_L, 1|\lambda)$ are the joint probabilities that the observation state $O_L$ is followed by 0 or 1, respectively, in the next state.

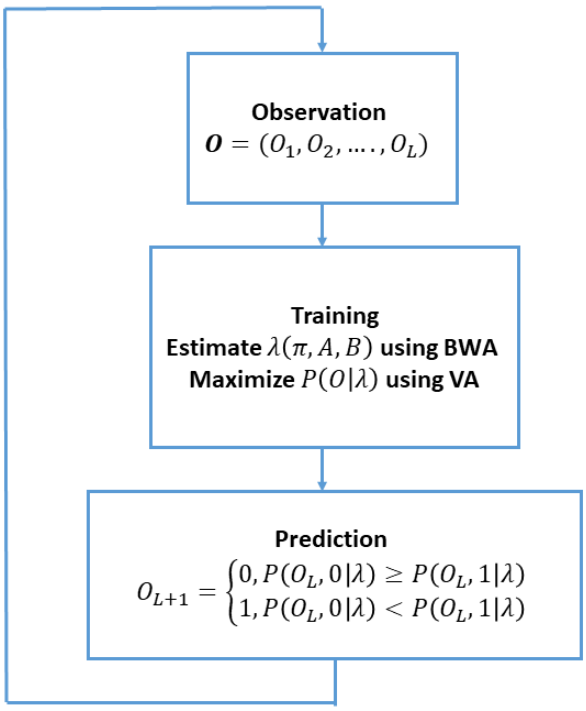


**Figure 2.3:** HMM predictor model.

#### 2.3.1.1 HMM Training

The Baum-Welch algorithm (BWA) is used to estimate $\lambda(\pi, A, B)$ and the Viterbi algorithm (VA) is used to train the model. The following variables are defined for the BWA.

- Forward variable $\alpha_l(i)$ is the probability of observing a partial sequence $(O_1, O_2, \ldots, O_l)$ such that $S_l$ at state $i$, where $\alpha_l(i) = P(O_1, O_2, \ldots, O_L, S_l = i|\lambda)$ $i \in \{0, 1\}$.
- Backward variable $\beta_l(i)$ is the probability of observing a partial sequence $(O_{l+1}, O_{l+2}, \ldots, O_L)$ such that $S_l$ at state $i$, where $\beta_l(i) = P(O_{l+1}, O_{l+2}, \ldots, O_L, S_l = i|\lambda)$ $i \in \{0, 1\}$.

- $\xi_l(i,j)$ is the probability of being in state $i$ at time $l$ and in state $j$ at time $l+1$.
- $\gamma_l(i,j)$ is the probability of being in state $i$ at time $l$ given the observation sequence $O$.
- $\widehat{a_{ij}}$ is the re-estimation of $a_{ij}$.
- $\widehat{b_{jk}}$ is the re-estimation of $b_{jk}$.
- $\widehat{\pi_i}$ is the re-estimation of $\pi_i$.

$\widehat{a_{ij}}$, $\widehat{b_{jk}}$ and $\widehat{\pi_i}$ are calculated in terms of $\xi_l(i,j)$ and $\gamma_l(i,j)$ as follows

$$\widehat{a_{ij}} = \frac{\sum_l \xi_l(i,j)}{\sum_l \sum_j \xi_l(i,j)} \tag{2.6}$$

$$\widehat{b_{jk}} = \frac{\sum_{l,O_l=k} \gamma_l(i,j)}{\sum_l \gamma_l(i,j)} \tag{2.7}$$

$$\widehat{\pi_i} = \gamma_1(i) \tag{2.8}$$

The re-estimation of $\lambda(\pi, A, B)$ is done until the maximum number of iterations or the maximum of $P(O|\lambda)$ is reached. $P(O|\lambda)$ is calculated as function of $\alpha_l(i)$. $\alpha_l(i)$ and $\beta_l(i)$ are calculated as shown in Table 2.1. $\xi_l(i,j)$ and $\gamma_l(i,j)$ are calculated as follows

$$\xi_l(i,j) = \frac{\alpha_l(i)\, a_{ij}\, b_{j(O_{l+1})} \beta_{l+1}(j)}{P(O|\lambda)} \tag{2.9}$$

$$\gamma_l(i,j) = \sum_{j=0}^{1} \xi_l(i,j) \tag{2.10}$$

| Variable | Equation | |
|---|---|---|
| $\alpha_l(i)$ | Initialization | $\alpha_1(i) = \pi_i b_{i(1)} \quad 0 \leq i \leq 1$ |
| | Recursion | $\alpha_{l+1}(j) = [\sum_{i=0}^{1} \alpha_l(i)\, a_{ij}]\, b_{j(\mathrm{O}_{l+1})}\ 0 \leq i,j \leq 1,\ 1 \leq l \leq L-1$ |
| | Termination | $P(O\|\lambda) = \sum_{i=0}^{1} \alpha_L(i) \quad 0 \leq i \leq 1$ |
| $\beta_l(i)$ | Initialization | $\beta_L(i) = 1 \quad 0 \leq i \leq 1$ |
| | Recursion | $\beta_l(j) = \sum_{j=0}^{1} b_{j(O_{l+1})} \beta_{l+1}(j)\, a_{ij}\ , \quad 0 \leq i,j \leq 1,\ L-1 \geq l \geq 1$ |

**Table 2.1:** Calculation of the forward and backward variables.

### 2.3.1.2 HMM Prediction

To predict the next state, the joint probabilities $P(O_L, 0|\lambda)$ and $P(O_L, 1|\lambda)$ are calculated as follows

$$P(O_L, 0|\lambda) = \sum_{i=0}^{1} \alpha_{L+1}^{0}(i), \quad \alpha_{L+1}^{0}(i) = [\sum_{i=0}^{1} \alpha_L(i)\, a_{ij}]\, b_{j(O_{L+1}=0)} \tag{2.11}$$

$$P(O_L, 1|\lambda) = \sum_{i=0}^{1} \alpha_{L+1}^{1}(i), \quad \alpha_{L+1}^{1}(i) = [\sum_{i=0}^{1} \alpha_L(i)\, a_{ij}]\, b_{j(O_{L+1}=1)} \tag{2.12}$$

The HMM prediction result is then [13, 14, 15]

$$D_{L+1} = \begin{cases} 0, P(O_L, 0|\lambda) \geq P(O_L, 1|\lambda) \\ 1, P(O_L, 0|\lambda) < P(O_L, 1|\lambda) \end{cases} \tag{2.13}$$

### 2.3.2 Neural Network Based Prediction Using an MLP

A multilayer perceptron (MLP) is a feedforward ANN consisting of an input layer, an output layer and non-linear layers called hidden layers in between. Each layer is fully connected to the next layer [8, 13, 14], as shown in Figure 2.4. The number of hidden layers

is $r$. A backpropagation (BP) learning algorithm is used to train the network. The input vector for the MLP predictor is the observation sequence $\boldsymbol{O} = (O_1, O_2, \ldots, O_L) \in \{0,1\}$. The observation sequence length $L$ defines the order of the MLP predictor. $S$ is unknown for the MLP predictor.

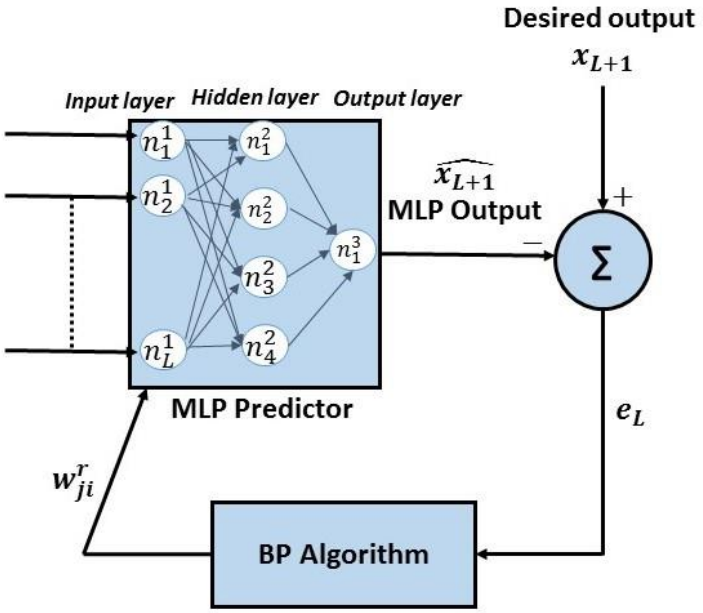


**Figure 2.4:** MLP predictor training.

The hidden layers consist of a number of nodes called neurons. Each neuron in a hidden layer is connected to each neuron in the next layer with a certain weight. Neurons are processing elements that calculate the weighted sum of the input (neuron connections from the previous hidden layer) and transform the sum through a non-linear function, as shown in Figure 2.5. $y_j^r$ is the output of neuron $j$ at the $r$th layer and represents a non-linear transform of $v_j^r$. $v_j^r$ is the weighted sum of the inputs using the adaptive weights $w_{ji}^r$. These inputs are the outputs from the neurons in layer $(r-1)$. $y_j^r$ and $v_j^r$ are calculated as follows

$$y_j^r = \frac{1-e^{-v_j^r}}{1+e^{-v_j^r}} \tag{2.14}$$

$$v_j^r = \sum_i y_i^{r-1} w_{ji}^r \tag{2.15}$$

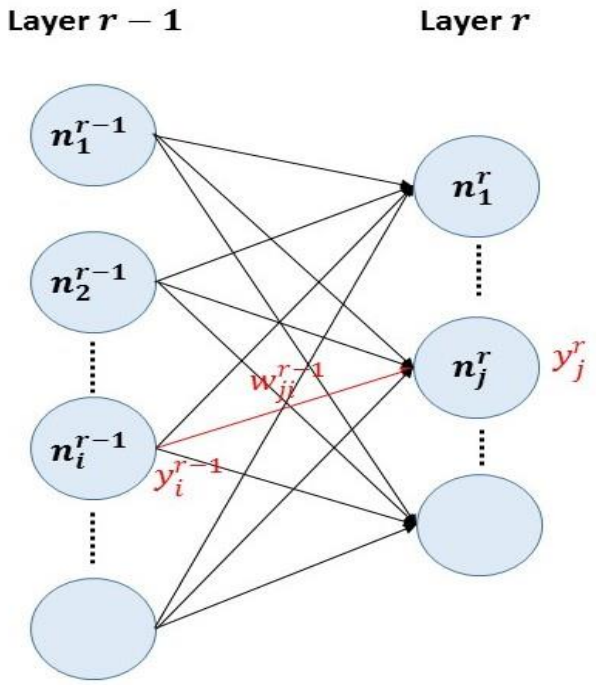


**Figure 2.5:** The computing process of a neuron.

The output from the weighted sum is in the range [-1, +1]. During training, the BP algorithm adapts the $w_{ji}^r$ to minimize the error between the MLP output $\widehat{x_{L+1}}$ and the desired output $x_{L+1}$

$$e_L = x_{L+1} - \widehat{x_{L+1}} \tag{2.16}$$

The MLP predictor is iterated until the minimum of the mean square error $E$ from previous iterations or a maximum number of iterations is reached [13, 14]

$$E = \frac{1}{2} \sum e_L^2 \tag{2.17}$$

After training is completed, the prediction decision is

$$G_{L+1} = \begin{cases} +1, \widehat{x_{L+1}} \geq 0 \\ -1, \widehat{x_{L+1}} < 0 \end{cases} \quad (2.18)$$

## 2.4 Cooperative Spectrum Prediction

CSP was proposed in [9, 10 ,11] to improve the prediction accuracy in comparison to SSP. The sharing of sensing or prediction results between cooperating SUs can be classified as centralized or decentralized [6], as shown in Figure 2.6. In centralized CSP, a central base station called a fusion center (FC) controls the CSP. In decentralized CSP, each SU shares its prediction or SS result with other SUs in its transmission range. Then, each SU combines the received results to make a decision. A centralized CSP is considered in this thesis.

Data fusion in CSP is the process of combining SSP decisions from cooperating SUs in pre-fusion CSP or the local SS decisions in post-fusion CSP. CSP data fusion is classified as soft fusion, quantized soft fusion or hard fusion [6]. In hard fusion, an SU sends only one bit $\in \{0, 1\}$, which represents the local prediction decision. A 0 indicates that the PU channel state is idle and a 1 indicates that the PU channel state is busy. In this thesis, only hard fusion is considered.

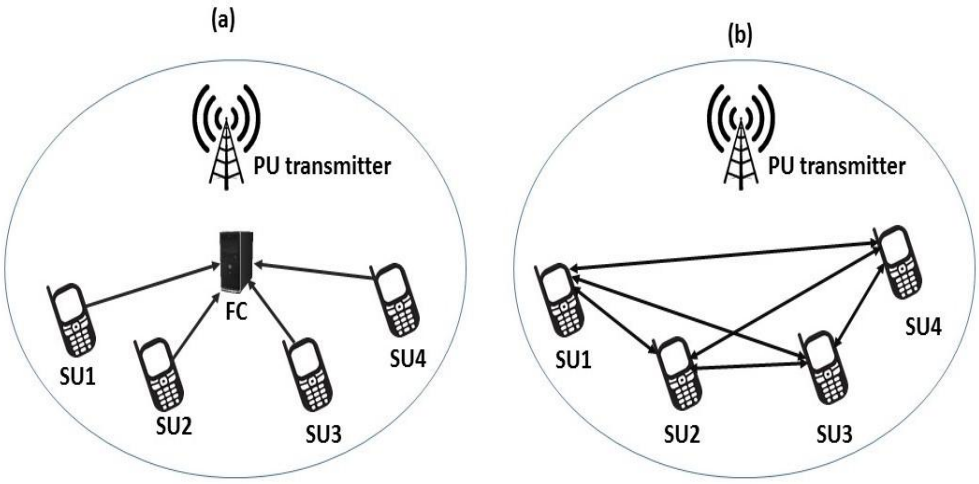


**Figure 2.6:** Classification of CSP, (a) centralized, and (b) distributed.

CSP can be performed in two ways: pre-fusion or post-fusion. In pre-fusion CSP [11], a number of SUs perform local spectrum prediction based on past SS results, and then send their binary SSP results (0 for an idle state or 1 for a busy state) to the FC. The FC uses one of the fusion rules AND, OR or majority rule to combine the received results, as shown in Figure 2.7. In post-fusion CSP [11], a number of SUs perform CSS. Then, The FC makes a prediction based on this and past CSS results as shown in Figure 2.8.

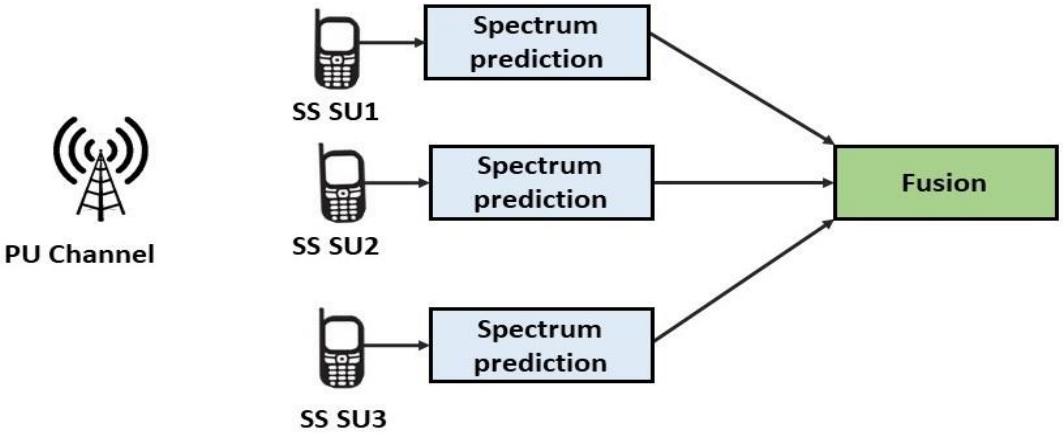


**Figure 2.7:** The pre-fusion cooperative spectrum prediction model.

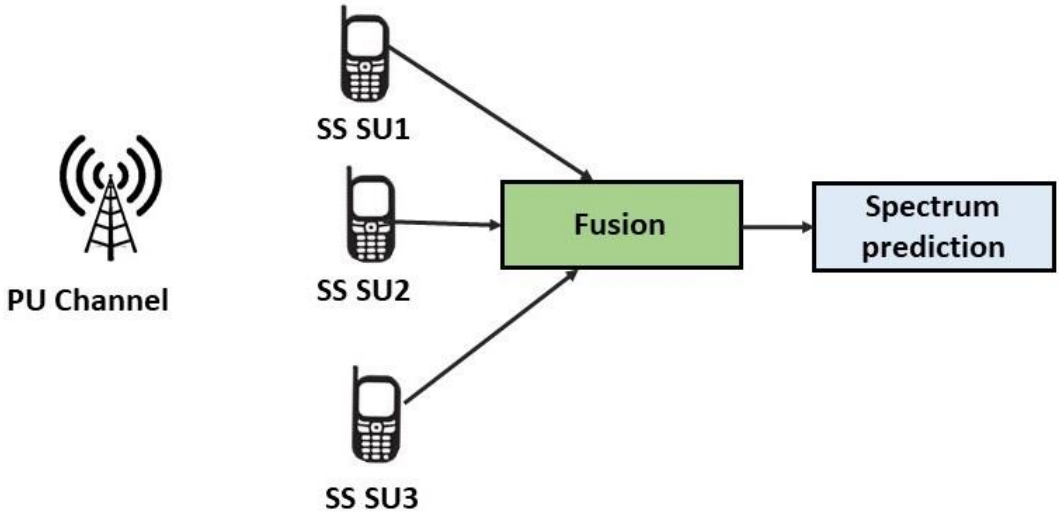


**Figure 2.8:** The post-fusion cooperative spectrum prediction model.

In this thesis, the cooperative gain is investigated for prediction accuracy improvement, spectrum efficiency improvement, and sensing energy reduction. Further, the overhead is investigated in terms of the extra prediction time and energy. However, the corresponding delay related to the prediction model and any computational complexity are not considered in this thesis.

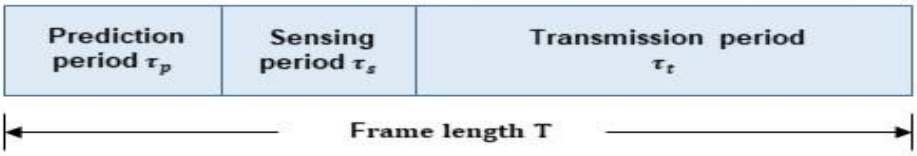


**Figure 2.9:** An SU frame.

For pre-fusion CSP and SSP, an SU frame has time period $T = \tau_p + \tau_s + \tau_t$ with prediction $\tau_p$, sensing $\tau_s$, and transmission $\tau_t$ periods as shown in Figure 2.9 [18]. During the prediction period, an SU performs local SSP on the PU channels using an HMM or MLP predictor. During the sensing period, an SU randomly selects one of the channels predicted to be idle to perform local SS. If the SS result is idle, the SU will start transmission in the transmission period. Otherwise, the SU waits until the next frame to repeat this process. A dedicated channel for reporting the prediction results is used for pre-fusion CSP with a total reporting time for the $M$ SUs of $M\tau_r$, where $\tau_r$ is the single user reporting time. This channel is also used to send the FC results to the $M$ SUs.

## 2.5 Spectrum Occupancy Prediction Performance

The spectrum occupancy prediction performance is evaluated using the following three parameters. The probability of prediction error for a busy channel state, which is denoted as $P_p^e(\text{Busy})$ for SSP and $\overline{P_P^e(\text{Busy})}$ for CSP. The probability of prediction error for an idle channel state, which is denoted as $P_p^e(\text{Idle})$ for SSP and $\overline{P_P^e(\text{Idle})}$ for CSP. The total probability of prediction error, which is denoted as $P_p^e(\text{Total})$ for SSP and $\overline{P_P^e(\text{Total})}$ for CSP. The goal is to reduce these prediction errors to ensure low PU interference and efficient SU utilization of the spectrum. For the HMM predictor we have

$$P_p^e(\text{Busy}) = P(D_{L+1} = 0 | S_{L+1} = 1) \tag{2.19}$$

$$P_p^e(\text{Idle}) = P(D_{L+1} = 1 | S_{L+1} = 0) \tag{2.20}$$

and

$$P_p^e(\text{Total}) = P(D_{L+1} \neq S_{L+1}) = P(S = 1)P_p^e(\text{Busy}) + P(S = 0)\, P_p^e(\text{Idle}) \tag{2.21}$$

and for the MLP predictor we have

$$P_p^e(\text{Busy}) \;=\; P(G_{L+1}=0|S_{L+1}=1) \tag{2.22}$$

$$P_p^e(\text{Idle}) \;=\; P(G_{L+1}=1|S_{\,L+1}=0) \tag{2.23}$$

and

$$P_p^e(\text{Total}) = P(G_{L+1} \neq S_{\,L+1}) = P(S=1)P_p^e(\text{Busy}) + P(S=0)\,P_p^e(\text{Idle}) \tag{2.24}$$

For pre-fusion CSP, the global prediction decision for the HMM predictor is

$$F \;= \begin{cases} 1, \; \sum_{i=1}^{M} D_{L+1}^i \geq Z \\ 0, \; \sum_{i=1}^{M} D_{L+1}^i < Z \end{cases} \tag{2.25}$$

and the global prediction decision for the MLP predictor is

$$F \;= \begin{cases} 1, \; \sum_{i=1}^{M} G_{L+1}^i \geq Z \\ 0, \; \sum_{i=1}^{M} G_{L+1}^i < Z \end{cases} \tag{2.26}$$

where $Z = \frac{M}{2}$ for the majority rule, $Z = M$ for the AND rule, and $Z = 1$ for the OR rule. With homogeneous SUs, $P_m^i$=$P_m$ and $P_f^i$=$P_f$, so that $D_{L+1}^i$= $D_{L+1}$ and $G_{L+1}^i$= $G_{L+1}$, where the superscript *i* denotes SU $i$. The probability of a cooperative prediction error for a *busy* channel state is

$$\overline{P_P^e(\text{Busy})} = P(F=0|S_{L+1}=1) = 1 - \sum_{i=Z}^{M}\binom{M}{Z} \; (1-P_p^e(\text{Busy}))^Z P_p^e(\text{Busy})^{M-Z} \tag{2.27}$$

and the probability of a cooperative prediction error for an idle channel state is

$$\overline{P_P^e(\text{Idle})} = P(F=1|S_{L+1}=0) = \sum_{i=Z}^{M}\binom{M}{Z} \; (P_P^e(\text{Idle}))^Z \; (1-P_P^e(\text{Idle}))^{M-Z} \tag{2.28}$$

The total probability of a cooperative prediction error is then

$$\overline{P_p^e(Total)} = P(S=1)\overline{P_P^e(Busy)} \; + P(S=0)\overline{P_P^e(Idle\,)} \tag{2.29}$$

# Chapter 3

# CRN Performance with Cooperative Spectrum Prediction

## 3.1 Previous Work

The prediction accuracy with SSP has been improved using machine learning techniques such as neural networks (NNs) and hidden Markov models (HMMs). In [16], a HMM-based spectrum occupancy predictor was proposed using measured data and compared with other prediction methods. The results obtained show that the HMM predictor outperforms both the *k*th order Markov model and first nearest neighbor predictors. In [10], a coalition game based approach was proposed for CSP in multi-PU CRNs to improve the prediction accuracy compared to SSP. In [11], the performance of both pre-fusion and post-fusion CSP was investigated, and an optimal CSP algorithm was proposed to minimize the prediction error. In [9], a pre-fusion homogeneous CSP was proposed using a HMM predictor. In this case, homogeneous CSP means the SUs have the same prediction accuracy. It was shown that majority rule based CSP provides better prediction accuracy than SSP. In [9, 10, 11], the focus was only on the CSP prediction accuracy improvement compared to SSP, and the EE and SE were not considered.

For SSP, the results in [13] showed that $P_p^e(\text{Busy})$ and $P_p^e(\text{Total})$ for SSP vary as a function of PU channel occupancy. In [11], the performance of different prediction methods was investigated as a function of PU channel occupancy. $P_p^e(\text{Total})$ was a maximum at 50% PU channel occupancy and a minimum at 10% and 90% PU channel

occupancy. In addition, $\overline{P_P^e(\text{Total})}$ for CSP was evaluated for both post-fusion and pre-fusion CSP as a function of SNR and as function of $P_p^e(\text{Total})$ for SSP. In [10], $\overline{P_P^e(\text{Total})}$ for CSP in a coalition game was investigated as a function of the number of PUs and SUs. In [9], $\overline{P_P^e(\text{Total})}$ was investigated as a function of the probability of SS error.

The impact of prediction time and prediction energy on the EE with SSP was investigated in [17], but no SS errors were assumed. Moreover, the SE improvement with SSP and the corresponding reduction in sensing energy were investigated in [13, 16, 17-20]. In [16], the sensing energy consumption was investigated for an HMM predictor. The results showed a reduction in sensing time and energy of up to 66% compared to TSS. In [18], the SE with SSP was investigated. The results showed an improvement compared to TSS in high traffic CRNs. In [13], the performance of MLP and HMM predictors was investigated and the improvement in SE and the reduction in sensing energy compared to TSS were examined. In [19], the SE of energy harvesting CRNs was examined. In [18], a constant prediction error ($P_p^e\ (\text{Total}) = constant$) for different traffic intensities was used to study the SE with SSP. In [19], $P_p^e(\text{Busy}) = P_p^e(\text{Idle}) = P_p^e\ (\text{Total}) = constant$ was used to investigate the SE. However, this assumption is not practical according to the SSP performance analysis in [13]. Further, the SE and EE with CSP and the effect of $P_p^e(\text{Busy})$ and $P_p^e(\text{Idle})$ on the SE were not investigated. The tradeoff between the EE and SE with CSS was investigated in [5], and it was shown that improving the EE decreases the SE. However, the SE-EE tradeoff with SSP and CSP has not been investigated.

In this thesis, the prediction performance of pre-fusion CSP is investigated as a function of the PU channel occupancy. This is done for different fusion rules using both

HMM and MLP predictors. $\overline{P_p^e(\text{Busy})}$ and $\overline{P_p^e(\text{Idle})}$ were not considered in [9, 10, 11]. $\overline{P_p^e\ (\text{Total})}$ was considered as a function of the number of PUs and SUs in [9], as function of the SNR and $P_p^e(\text{Total})$ in [10], and as a function of the probability of SS error in [11]. In this thesis, $\overline{P_p^e\ (\text{Total})}$, $\overline{P_p^e(\text{Busy})}$ and $\overline{P_p^e(\text{Idle})}$ are investigated as a function of the PU channel occupancy. Instead of assuming $P_p^e(\text{Busy}) = P_p^e(\text{Idle}) = P_p^e\ (\text{Total}) = constant$ as in [17] to investigate the SE with SSP, different $\overline{P_p^e(\text{Busy})}$ and $\overline{P_p^e(\text{Idle})}$ are considered in the CSP SE and EE evaluation. Further, the SE and EE with CSP is compared to the SE and EE with SSP and TSS. Only the prediction performance for CSP was investigated in [9, 10, 11]. Further, the effect of $P_p^e(\text{Busy})$ and $P_p^e(\text{Idle})$ on the SE is investigated as only $P_p^e(\text{Total})$ was considered in [17, 18].

## 3.2 System Model

A centralized CRN is considered which consists of $M$ SUs that cooperate in the pre-fusion CSP process and $N$ PUs each with distinct channels as illustrated in Figure 3.1. Only one SU from the cooperating group is allowed to transmit so there are no SU collisions.

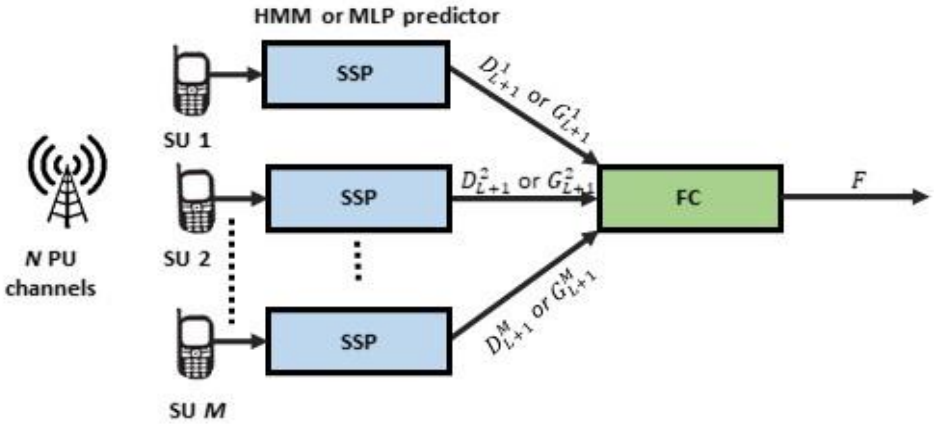


**Figure 3.1:** The system model for CSP.

PU activity is assumed to be independent. The PU traffic is modeled as a two-state Markov process defined by $(\mu, \theta)$ where $\mu$ is the probability of remaining in the idle state and $\theta$ is the probability of remaining in the busy state. The PU true channel state is $S \in \{0, 1\}$. In addition, the channel is busy with probability $P_b = P(S = 1)$ and idle with probability $P_i = P(S = 0)$. $P_b$ is the probability of PU channel occupancy. The SUs use an energy detector to sense the PU channels. $O_l$ is the sensing channel state at time slot $l$. In this thesis, the SUs are assumed to be homogeneous with $P_m^i = P_m$ and $P_f^i = P_f$, so that $D_{L+1}^i = D_{L+1}$ and $G_{L+1}^i = G_{L+1}$, where the superscript $i$ denotes SU $i$ , $1 \leq i \leq M$.

The SE for a SU in a CRN [18] is given in Table 1. The SE is $C_0$ when the SU transmits and the PU is idle (the idle channel is detected correctly so the SU does not interfere with the PU). The corresponding signal to noise ratio (SNR) at the receiver is $\mathrm{SNR_s}$. The SE is $C_1$ when the SU transmits and the PU is busy (the busy channel is not detected so the SU interferes with the PU). The SNR of the PU signal at the receiver is $SNR_p$ [14].

| True Channel State | Sensing Channel State | SE |
|---|---|---|
| 0 | 0 | $C_0 = \frac{\tau_t}{T} \log_2(1 + SNR_s)$ |
| 1 | 0 | $C_1 = \frac{\tau_t}{T} \log_2(1 + \frac{SNR_s}{1+SNR_p})$ |

**Table 3.1:** The SU spectrum efficiency.

## 3.3 Performance Analysis

### 3.3.1 Spectrum Prediction Performance

The SSP is evaluated using HMM and MLP predictors. The performance of each predictor is evaluated using $P_p^e(\text{Busy})$, $P_p^e(\text{Idle})$ and $P_p^e(\text{Total})$ as given in Section 2.3. Further, the CSP is evaluated using HMM and MLP predictors. The performance of each predictor is evaluated using $\overline{P_p^e(\text{Busy})}$, $\overline{P_p^e(\text{Idle})}$ and $\overline{P_p^e(\text{Total})}$ as given in Section 2.3.

### 3.3.2 Spectrum Efficiency with Cooperative Spectrum Prediction

In this section, the effect of $\overline{P_P^e(\text{Busy})}$ and $\overline{P_P^e(\text{Idle})}$ on the SE with CSP is considered. There are four possibilities, correct prediction of an idle channel state $\left(1-\overline{P_P^e(\text{Idle})}\right)$, wrong prediction of an idle channel state $\overline{P_P^e(\text{Idle})}$, wrong prediction of a busy channel state $\overline{P_P^e(\text{Busy})}$, and correct prediction of a busy channel state $\left(1-\overline{P_P^e(\text{Busy})}\right)$. The joint probabilities of true and predicted channel states are given in Table 3.2.

| True Channel State | Predicted State | Probability |
|---|---|---|
| Idle | Idle | $P_i\left(1-\overline{P_P^e(\text{Idle})}\right)$ |
| Idle | Busy | $P_i\,\overline{P_P^e(Idle)}$ |
| Busy | Idle | $P_b\,\overline{P_P^e(\text{Busy})}$ |
| Busy | Busy | $P_b\left(1-\overline{P_P^e(\text{Busy})}\right)$ |

**Table 3.2:** Joint probabilities of true and predicted channel states.

The probability of predicting an idle state for a PU channel is

$$P_p^0 = P_i\,(1 - \overline{P_P^e(\text{Idle})}) + P_b\,\overline{P_P^e(\text{Busy})} \tag{3.1}$$

and the probability of predicting a busy state for a PU channel is

$$P_p^1 = P_i\,\overline{P_P^e(\text{Idle})} + P_b\,(1 - \overline{P_P^e(\text{Busy})}) \tag{3.2}$$

For a CRN with $N$ PUs, the probability of predicting $k$ idle channels is $C_N^k (P_p^0)^k (P_p^1)^{N-k}$. Therefore, the probability of predicting at least one idle channel is

$$P_N^0 = \sum_{k=1}^{N} C_N^k\ (P_p^0)^k (P_p^1)^{N-k} \tag{3.3}$$

and the probability of predicting that every channel is busy is

$$P_N^1 = \ C_N^0\ (P_p^0)^0 (P_p^1)^{N-0} = (P_p^1)^N \tag{3.4}$$

The joint probabilities for the true, predicted and sensed states are listed in Table 3.3. For SE and EE evaluation with SSP, $\overline{P_P^e(\text{Idle})}$ and $\overline{P_P^e(\text{Busy})}$ are replaced by $P_p^e(\text{Idle})$ and $P_p^e(\text{Busy})$, respectively.

| True Channel State | Predicted State | Sensed State | Probability |
|---|---|---|---|
| Idle | Idle | Idle | $P_1 = \dfrac{(1-P_f)P_i\,(1-\overline{P_P^e(\text{Idle})})}{P_p^0}\ P_N^0$ |
| Idle | Idle | Busy | $P_2 = \dfrac{P_f P_i\,(1-\overline{P_P^e(\text{Idle})})}{P_p^0}\ P_N^0$ |
| Idle | Busy | Idle | $P_3 = \dfrac{(1-P_f)\,P_i\ \overline{P_P^e(\text{Idle})}}{P_p^1}\ P_N^1$ |
| Idle | Busy | Busy | $P_4 = \dfrac{P_f\ P_i\,(1-\overline{P_P^e(\text{Idle})})}{P_p^1}\ P_N^1$ |

| | | | |
|---|---|---|---|
| Busy | Idle | Idle | $P_5 = \frac{(1-P_d)P_b\,\overline{P_P^e(\text{Busy})}}{P_p^0}\,P_N^0$ |
| Busy | Idle | Busy | $P_6 = \frac{P_d\,P_b\,\overline{P_P^e(\text{Busy})}}{P_p^0}\,P_N^0$ |
| Busy | Busy | Idle | $P_7 = \frac{(1-P_d)\,P_b\,\left(1-\overline{P_P^e(\text{Busy})}\right)}{P_p^1}\,P_N^1$ |
| Busy | Busy | Busy | $P_8 = \frac{P_d\;P_b\;\left(1-\overline{P_P^e(\text{Busy})}\right)}{P_p^1}\,P_N^1$ |

**Table 3.3:** Joint probabilities of true, predicted and sensed channel states.

An SU will sense only one channel from the channels that are predicted to be idle and transmit if the sensed state is idle. Therefore, the average SE is

$$SE_{avg} = P_1\,C_0 + P_5\,C_1 \quad \text{bits/s/Hz} \tag{3.5}$$

and the normalized SE is

$$SE_{norm} = \frac{SE_{avg}}{SE_{upper}} \tag{3.6}$$

where

$$SE_{upper} = P_i\;C_0 + P_b\;C_1 \quad \text{bits/s/Hz} \tag{3.7}$$

### 3.3.3 Energy Efficiency with Cooperative Spectrum Prediction

To investigate the EE with CSP, the average energy consumption for CSP is expressed as a function of the time and power consumption. The prediction power, reporting power, sensing power, and transmit power for an SU are denoted by $P_p$ , $P_r$ , $P_s$ and $P_T$, respectively. Then the average energy consumption with CSP is

$$E_{avg-CSP} = M(\tau_p P_p + \tau_r P_r) + (P_1 + P_5)\tau_t P_T + (P_1 + P_2 + P_5 + P_6)\tau_s P_s \quad (3.8)$$

the average energy consumption with SSP is

$$E_{avg-SSP} = \tau_p P_p + (P_1 + P_5)\tau_t P_T + (P_1 + P_2 + P_5 + P_6)\tau_s P_s \quad (3.9)$$

and the average energy consumption with TSS is

$$E_{avg-TSS} = ((1 - P_f)P_i + (1 - P_d)P_b)\tau_t P_T + \tau_s P_s \quad (3.10)$$

The EE of the CRN is then

$$EE = \frac{SE_{avg}}{E_{avg}/T} \quad \text{bits/Joule/Hz} \quad (3.11)$$

# Chapter 4

## Performance Results

To evaluate the CRN performance with CSP, simulation using Matlab was conducted for the HMM and MLP predictors. Then, the SE and EE evaluation with CSP are evaluated. The simulation parameters for the HMM and MLP predictors are listed in Table 4.1. In the simulation, the HMM and MLP predictors are trained with 100 slots, and tested on the binary sequence of 30,000 slots under each PU traffic occupancy setting from 10% to 90%. The training of MLP predictor is done only once but the training of HMM predictor is repeated for every test. The input for both predictors was the 30,000 slots of SS results with $P_m = 0.1$ and $P_f = 0.1$. The prediction result was compared with the two-state Markov process PU traffic for different 9 PU traffic occupancies from 10% to 90%. CSP was evaluated using the AND, OR and majority rules. The system parameters for the SE are the same as in [18], except for $\tau_s$ and $\tau_p$ which are given in the table. Further, $P_p^e(Busy)$, $P_p^e(Idle)$ and $P_p^e\ (Total)$ were obtained from the HMM and MLP prediction results. The system parameters for SE and EE are also given in Table 4.1. $N$, $T$, $SNR_s$ and $SNR_p$ are the same as in [14], and the values of $P_p$, $P_r$, $P_s$, $P_T$, $\tau_t$, $\tau_s$, $\tau_p$ and $\tau_r$ are the same as in [17].

| Parameter | Value | Parameter | Value |
|---|---|---|---|
| $P_m$ | 0.1 | $SNR_s$ | 20 dB |
| $P_f$ | 0.1 | $SNR_p$ | -15 dB |
| $P_b$ | 0.1 to 0.9 | $P_p$ | 20 mw |
| $L$ | 100 for HMM and MLP | $P_r$ | 10 mw |
| $r$ | 2, each with 25 neurons | $P_s$ | 110 mw |
| $M$ | 10 | $P_T$ | 160 mw |
| $N$ | 10 | $\tau_t$ | 85 ms |
| $T$ | 100 | $\tau_s$ | 10 ms |
| $\tau_r$ | 100 μs | $\tau_p$ | 5 ms |

**Table 4.1:** The system parameters.

## 4.1 Prediction Performance

The CSP performance was evaluated for the three fusion rules. Figures 4.1 and 4.2 show $P_p^e(\text{Total})$ and $\overline{P_p^e(\text{Total})}$ as a function of PU channel occupancy from 10% to 90% with the HMM and MLP predictors, respectively. For the HMM and MLP predictors, $P_p^e(\text{Total})$ for SSP is the smallest when the PU channel occupancy is 90% and 10%, and a maximum for a channel occupancy around 50%. However, $P_p^e(\text{Total})$ for the HMM predictor is smaller than with the MLP predictor for SSP and CSP with all three fusion rules. Thus, the HMM predictor provides better performance than the MLP predictor, but the computational complexity of the HMM predictor is higher [8]. This is due to the number of computations required for the training. The MLP predictor is trained only once whereas the HMM predictor is trained repeatedly. In the simulations, the HMM training is done for 30,000 slots. The number of computations after training is a function of the number of states in the HMM. Here, the number of calculations after training is 1225 for the MLP

predictor and 400 for the HMM predictor, so it is higher for the MLP. The majority rule provides better performance than SSP and the other fusion rules. On the other hand, the AND and OR rules have the worst performance in the high and low traffic cases, respectively.

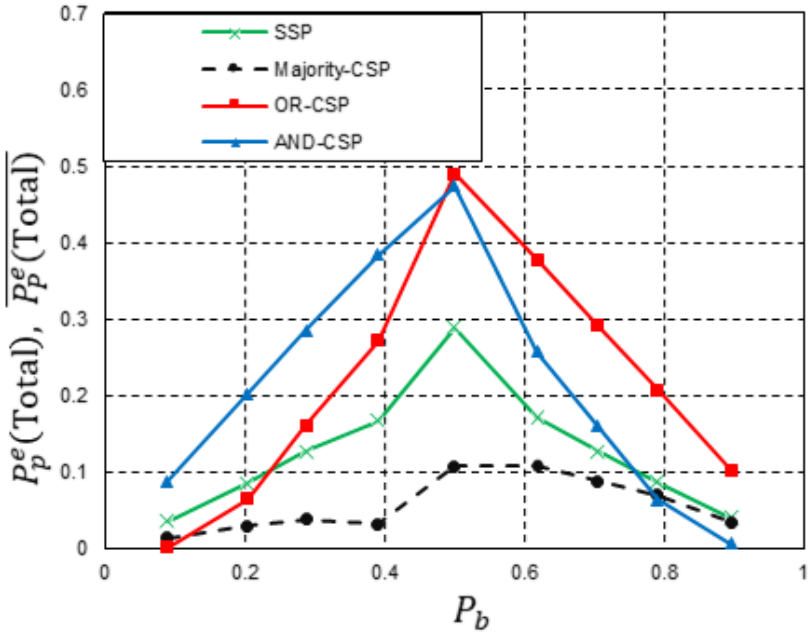


**Figure 4.1:** $P_p^e(\text{Total})$ and $\overline{P_p^e(\text{Total})}$ versus PU channel occupancy with the HMM predictor.

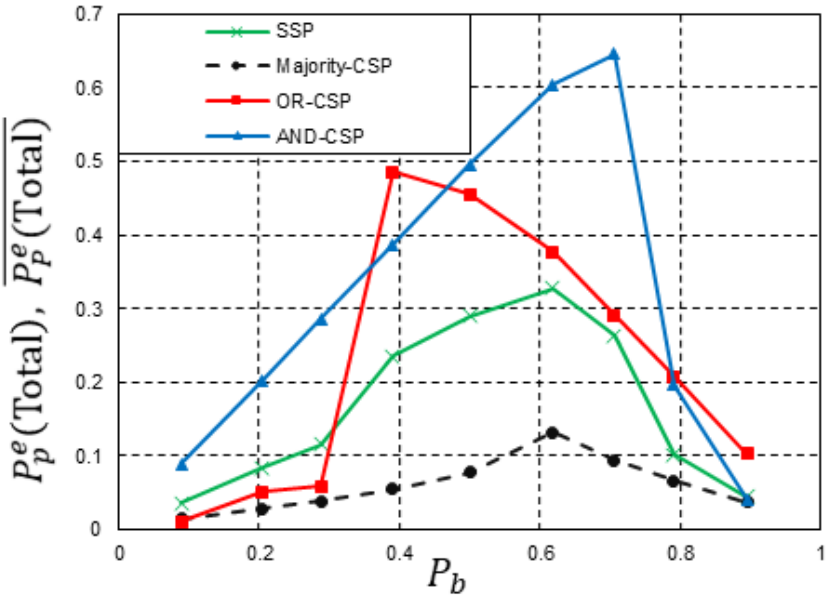


**Figure 4.2:** $P_p^e(\text{Total})$ and $\overline{P_p^e(\text{Total})}$ versus PU channel occupancy with the MLP predictor.

Figures 4.3 and 4.4 show $P_p^e(\text{Busy})$ and $P_p^e(\text{Idle})$ for CSP, respectively. $\overline{P_p^e(\text{Busy})}$ and $\overline{P_p^e(\text{Idle})}$ versus PU channel occupancy with all fusion rules compared to SSP are also given for the HMM and MLP predictors. For SSP, $P_p^e(\text{Idle})$ increases and $P_p^e(\text{Busy})$ decreases as the PU channel occupancy increases. In the low traffic case ($P_b < 0.5$), the probability of having an idle state is higher than in high traffic case ($P_b > 0.5$) and vice versa. Therefore, $P_p^e(\text{Busy})$ and $P_p^e(\text{Idle})$ are lowest when the PU channel occupancy is 90% and 10%, respectively. In general, $P_p^e(\text{Idle})$ with the MLP predictor is slightly lower than $P_p^e(\text{Idle})$ with the HMM predictor by an average of 2%. Conversely, $P_p^e(\text{Busy})$ with the HMM predictor is lower than $P_p^e(\text{Busy})$ with the MLP predictor by an average of 20%. For pre-fusion CSP, $\overline{P_p^e(\text{Busy})}$ with the OR rule is lower than with SSP

and other fusion rules, but $\overline{P_p^e(\text{Idle})}$ is the highest. Further, $\overline{P_p^e(\text{Idle})}$ with the AND rule is lower than with other fusion rules or SSP, but $\overline{P_p^e(\text{Busy})}$ is the highest. As a result, the majority rule provides a good tradeoff between $\overline{P_p^e(\text{Busy})}$ and $\overline{P_p^e(\text{Idle})}$ compared with the AND and OR rules and SSP.

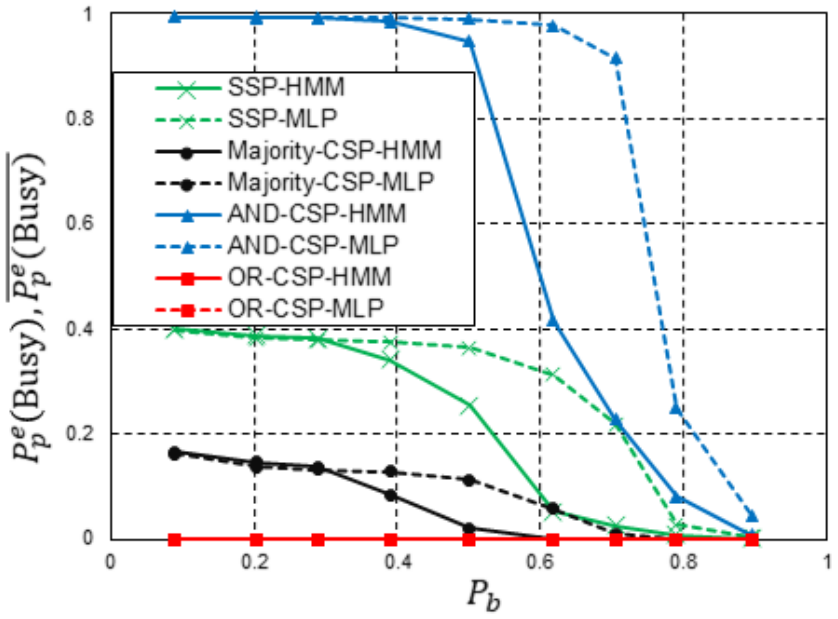


**Figure 4.3:** $P_p^e(\text{Busy})$ and $\overline{P_p^e(\text{Busy})}$ versus PU channel occupancy for the HMM and MLP predictors.

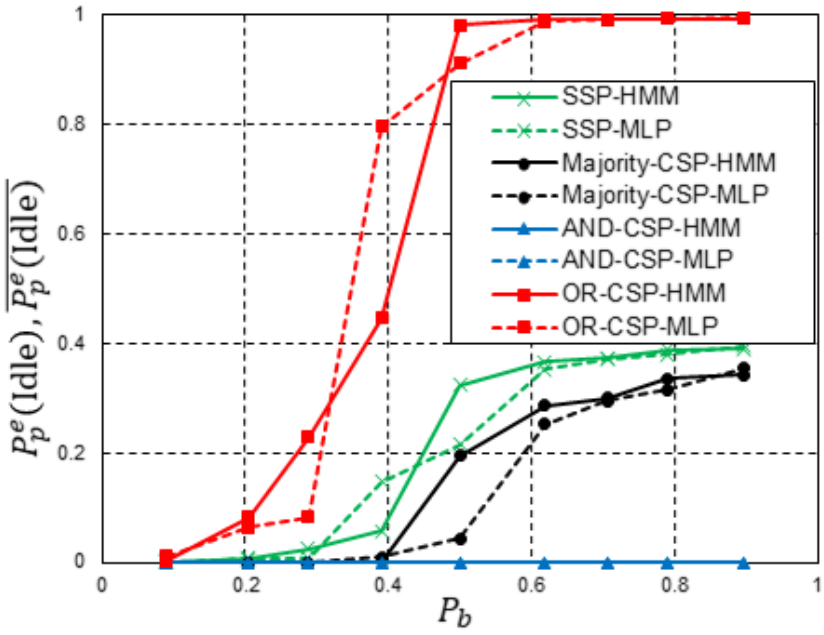


**Figure 4.4:** $P_p^e(\text{Idle})$ and $\overline{P_p^e(\text{Idle})}$ versus PU channel occupancy for the HMM and MLP predictors.

### 4.1.1 Spectrum Efficiency with Cooperative Spectrum Prediction

The effect of $P_p^e(\text{Busy})$ and $P_p^e(\text{Idle})$ for SSP and $\overline{P_p^e(\text{Busy})}$ and $\overline{P_p^e(\text{Idle})}$ for CSP on the SE is evaluated using the previous HMM and MLP prediction results. $SE_{norm}$ versus PU channel occupancy is shown in Figures 4.5 and 4.6 for the HMM and MLP predictors, respectively. In comparison to TSS, there is a significant improvement in $SE_{norm}$ with majority rule based CSP. The average improvement is 25% and 150% for the low and high traffic cases, respectively. In the low traffic case, $SE_{norm}$ with the OR rule is higher than with the other fusion rules and SSP. On the other hand, $SE_{norm}$ with the AND rule and TSS are the worst. $SE_{norm}$ for the OR rule is higher than with the majority rule when $P_b <$ 0.4, even though $\overline{P_p^e(\text{Total})}$ with majority rule is lower than with the OR rule. Thus,

$\overline{P_p^e(\text{Total})}$ is not a good indicator of SE. In the high traffic case, $SE_{norm}$ with the majority rule is higher than the other fusion rules. On the other hand, $SE_{norm}$ with the OR rule and TSS is the worst. In general, $SE_{norm}$ with the HMM predictor is higher than $SE_{norm}$ with the MLP predictor for CSP with all fusion rules and SSP. However, the MLP predictor provides lower values of $P_p^e(\text{Idle})$. The difference in $SE_{norm}$ between SSP and majority rule CSP becomes small when $P_b > 0.8$. $SE_{norm}$ with SSP using $P_p^e(\text{Total}) = constant = 0.2$ as in [18] is also shown in Figures 4.5 and 4.6. This indicates that $SE_{norm}$ with majority rule based CSP is higher than these results and the difference increases as $P_b$ increases. However, $SE_{norm}$ with SSP using $P_p^e(\text{Busy})$ and $P_p^e(\text{Idle})$ from the HMM predictor is lower than with $P_p^e(\text{Total}) = constant = 0.2$ when $P_b < 0.5$ and higher when $P_b > 0.5$.

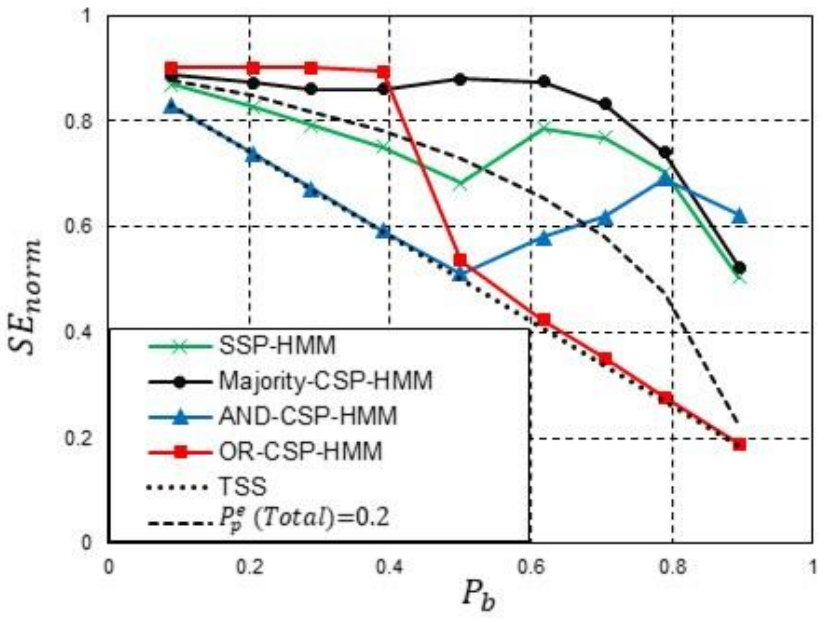


**Figure 4.5:** Normalized SE versus PU channel occupancy for the HMM predictor.

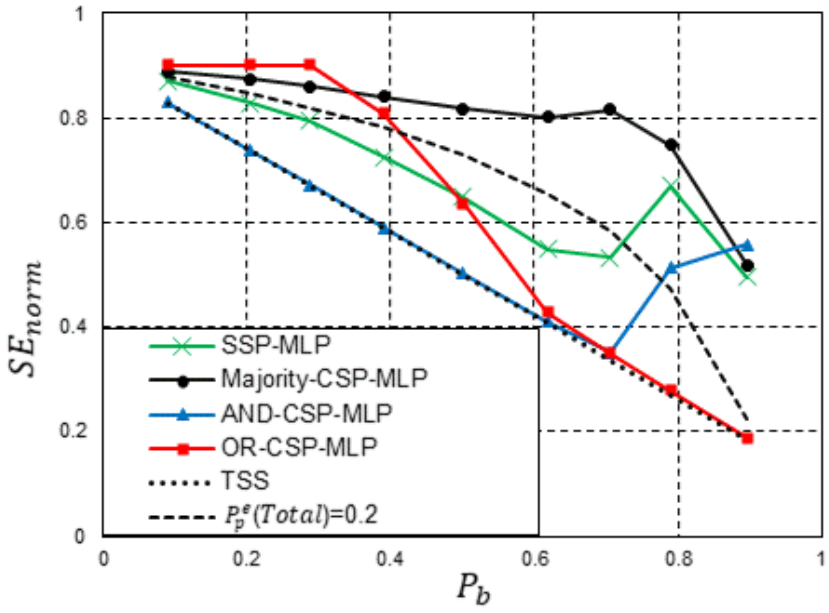


**Figure 4.6:** Normalized SE versus PU channel occupancy for the MLP predictor.

Figure 4.7 shows $SE_{norm}$ as a function of $P_p^e(\text{Busy})$ and $P_p^e(\text{Idle})$ for $P_b = 0.3$ and 0.7. Three cases are considered, $P_p^e(\text{Busy}) = 0$, $P_p^e(\text{Idle}) = 0$, and $P_p^e(\text{Busy}) = P_p^e(\text{Idle})$. In general, there is a significant decrease in $SE_{norm}$ when $P_p^e(\text{Busy})$ and/or $P_p^e(\text{Idle})$ increase in high traffic compared to the lower traffic case. When $P_p^e(\text{Busy}) = 0$, $SE_{norm}$ slowly decreases from 0.9 to 0.66 and from 0.9 to 0.34 for $P_b = 0.3$ and $P_b = 0.7$, respectively, as $P_p^e(\text{Idle})$ decreases. When $P_p^e(\text{Idle}) = 0$, $SE_{norm}$ decreases from 0.9 to 0.66 and from 0.9 to 0.34 for $P_b = 0.3$ and $P_b = 0.7$, respectively, as $P_p^e(\text{Busy})$ increases. When $P_p^e(\text{Idle}) = P_p^e(\text{Busy})$, which is equivalent to the assumption used in [18, 19], $SE_{norm}$ decreases rapidly from 0.8 to 0.02 for $P_b = 0.3$ and 0.7, in comparison to the cases $P_p^e(\text{Busy}) = 0$ and $P_p^e(\text{Idle}) = 0$.

With prediction based spectrum sensing, the SUs only sense channels that are predicted to be idle. Increasing $P_p^e(\text{Busy}) = P(D_{L+1} = 0|S_{L+1} = 1)$ leads to increased sensing of busy channels, which will reduce the SE. This effect is greater in high traffic CRNs where the probability of choosing a busy channel is high. On the other hand, an increase in $P_p^e(\text{Idle}) = P(D_{L+1} = 1|S_{L+1} = 0)$ reduces the chances to utilize the spectrum, as the probability of choosing an idle channel is decreased. This has a greater effect in high traffic CRNs. Consequently, a reduction in $P_p^e(\text{Busy})$ increases the SE more compared to a reduction in $P_p^e(\text{Idle})$. This explains why $SE_{norm}$ for CSP with the OR rule is better than $SE_{norm}$ with the AND rule in low traffic as shown in Figures 4.5 and 4.6. Although $\overline{P_p^e(\text{Total})}$ for CSP with the majority rule is better than with the other fusion rules and SSP, $SE_{norm}$ with the OR and AND rules is better than $SE_{norm}$ with the majority rule when $P_b < 0.4$ and $P_b > 0.88$, respectively. Therefore, $P_p^e(\text{Busy})$ and $P_p^e(\text{Idle})$ may be better indicators of CRN SE performance than $P_p^e(\text{Total})$.

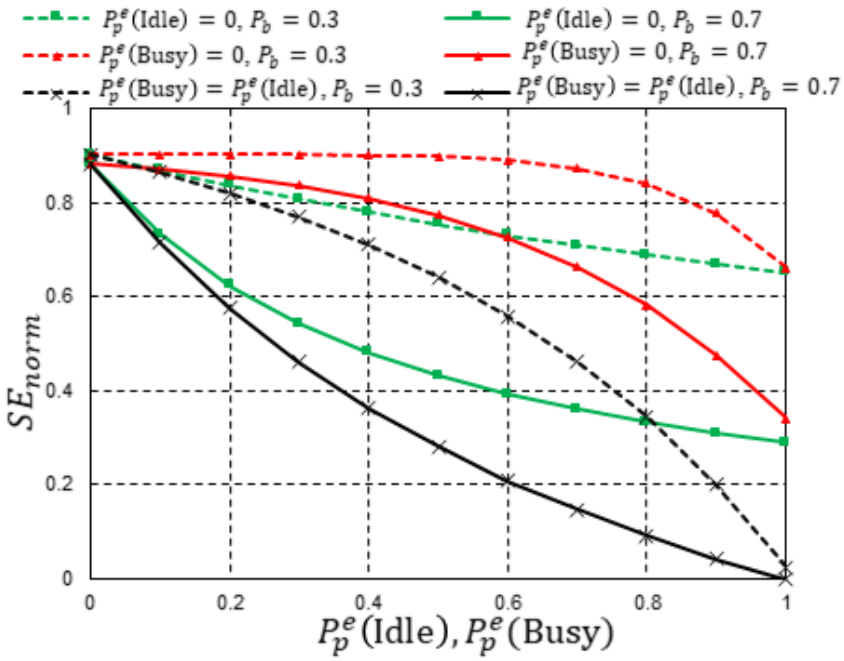


**Figure 4.7:** Normalized SE versus $P_p^e(\text{Idle})$ and $P_p^e(\text{Busy})$.

$SE_{norm}$ is compared for different numbers of PU in Figure 4.8. Only the HMM predictor is considered to investigate $SE_{norm}$ for SSP and CSP with the majority rule. As $N$ increases, $SE_{norm}$ increases for SSP and CSP because more channels can be used for transmission. Further, this increase started when $P_b \geq 0.4$. To explain this, the probability of predicting at least one idle channel $P_N^0$ is shown in Figure 4.9. Figure 4.9 shows that $P_N^0$ increases as $N$ increases. On the other hand, $P_N^0$ decreases as $P_b$ increses starting from 0.4. This is because the chance of having an idle channel decreases, so increasing $N$ increases the probability of more idle channels.

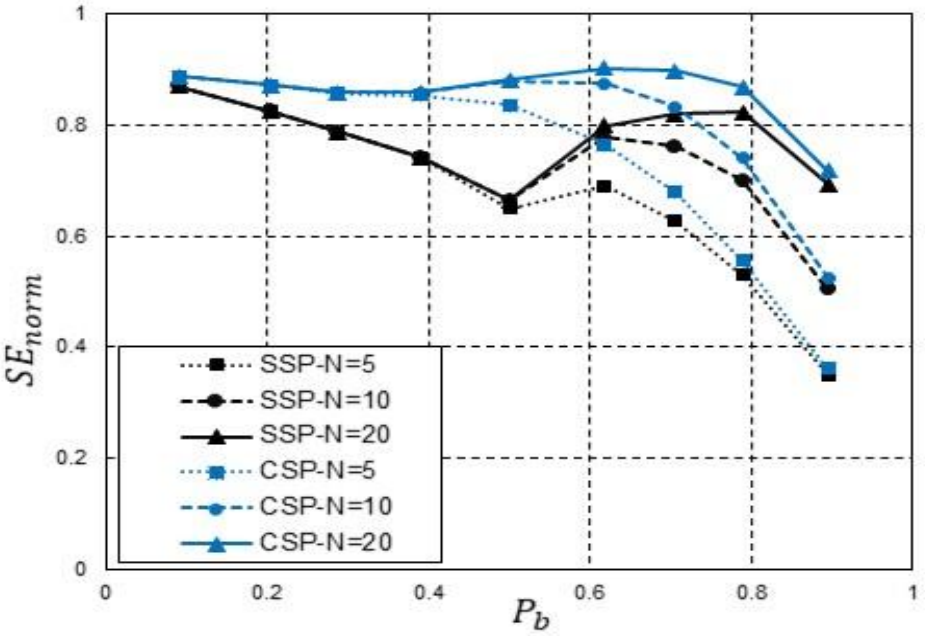


**Figure 4.8:** Normalized SE versus PU channel occupancy for $N$=5, 10 and 20.

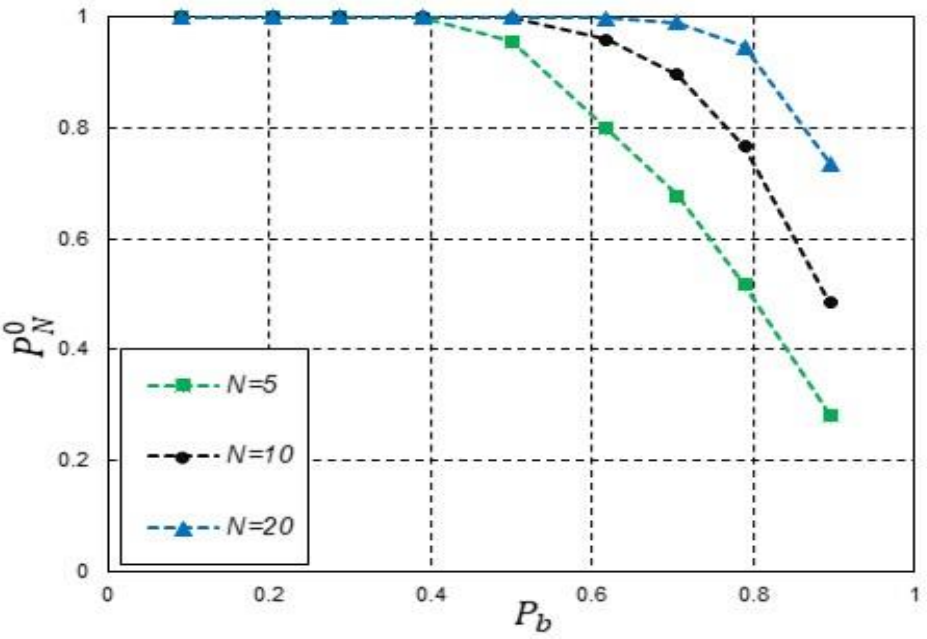


**Figure 4.9:** $P_N^0$ versus PU channel occupancy for $N$=5, 10 and 20.

### 4.1.2 Energy Efficiency with Cooperative Spectrum Prediction

In the previous section, the HMM predictor provided better results than the MLP predictor. Thus in this section, only the HMM predictor is considered to investigate the EE. The EE with CSP, SSP and TSS is shown in Figure 4.10. Although $SE_{norm}$ with majority rule based CSP was higher than with SSP, the EE with majority rule based CSP is lower than with SSP. This is due to the extra overhead required for SU cooperation. For this reason, increasing the number of cooperating SUs for CSP results in greater energy consumption and lower EE. In general, The EE with SSP is better than with TSS and majority rule based CSP. In the low traffic case ($P_b < 0.25$), the EE with TSS is better than with SSP. This is because the energy consumption with SSP degrades the EE compared to the improvement in SE. In the high traffic case ($P_b > 0.58$), the EE with majority rule based CSS is better than with TSS. This is because of the lower probability of having an idle PU channel in high traffic conditions. Random channel selection increases the sensing energy and transmit wait time which leads to poor SE and EE. On the other hand, SSP and CSP reduce the wait time which increases the SE. Nevertheless, the EE with CSP is lower than with SSP due to the higher power required for prediction. Thus, CSP improves the SE at a cost of increasing the prediction energy although the sensing energy is decreased compared to SSP and TSS.

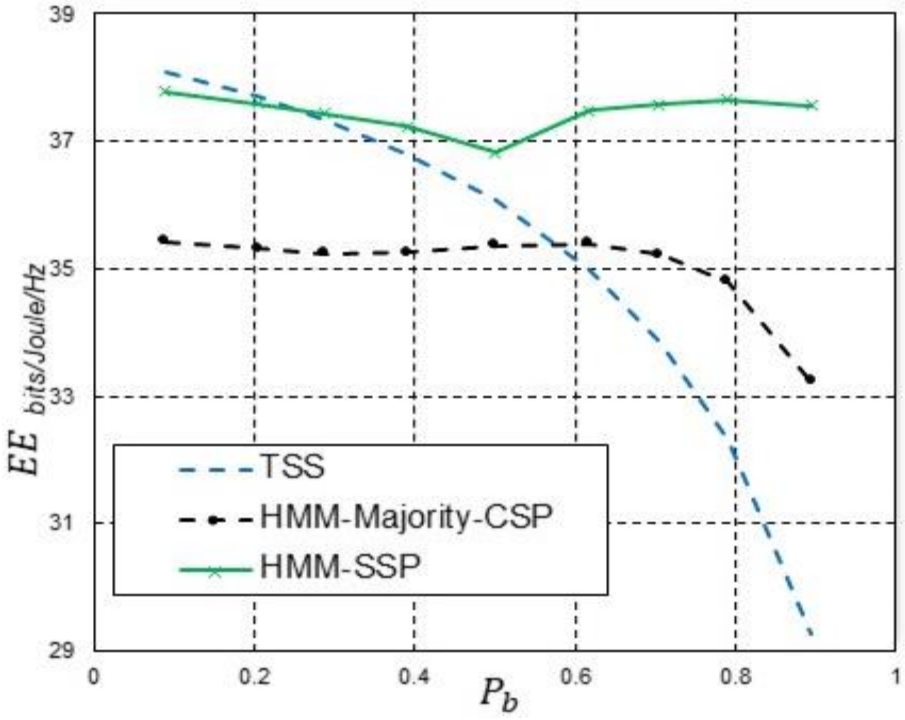


**Figure 4.10:** Energy efficiency versus PU channel occupancy.

# Chapter 5

# Conclusion and Future Work

## 5.1 Conclusion

Channel status prediction plays a vital role in effective spectrum utilization in cognitive radio networks (CRNs). Thus, cooperative spectrum prediction (CSP) was introduced to improve the prediction accuracy compared to single spectrum prediction (SSP). In this thesis, the performance of cooperative spectrum prediction using HMM and MLP predictors was investigated as a function of PU channel occupancy. In addition, pre-fusion cooperation spectrum prediction was compared for OR, AND and the majority rule fusion schemes. Further, the spectrum and energy efficiency of cooperative spectrum prediction were investigated, as well as the effect of a busy state and/or idle state prediction error on the spectrum efficiency were investigated. From the results in Section 4.2, the main conclusions of this thesis are as follows.

- The HMM predictor provides better performance than the MLP predictor.
- For $P_p^e(\text{Total})$, majority rule provides the best performance compared to SSP and the other fusion rules. On the other hand, the AND and OR rules have the worst performance in the high and low traffic cases, respectively.
- The majority rule provides a good tradeoff between $\overline{P_p^e(\text{Busy})}$ and $\overline{P_p^e(\text{Idle})}$ compared with the AND and OR rules and SSP.
- The SE with majority rule based CSP provides better performance than TSS.

- A reduction in $P_p^e(\text{Busy})$ increases the SE more compared to a reduction in $P_p^e(\text{Idle})$.
- The EE with majority rule based CSP is lower than with SSP.

## 5.2 Future Work

The following future work is proposed for CRNs.

- Extend the system model introduced in Section 3.3 by including post-fusion prediction based on cooperative spectrum sensing to mitigate the extra cooperative overhead introduced by this model (prediction time and prediction energy for all users).
- Parallel cooperative spectrum prediction can be introduced as an improvement for parallel cooperative spectrum sensing [21]. Parallel cooperative spectrum sensing has been proposed as a new sensing scheme to enhance sensing efficiency based on grouped SUs.
- Heterogeneous cooperative spectrum prediction can be studied for the case when the spectrum sensing performance ($P_m$ and $P_f$) is not the same for all SUs.
- Investigate the tradeoff between spectrum and energy efficiency in CSP following the work in [5] for CSS, as improving the SE will decrease the EE as shown in this thesis. Therefore, solving an optimization problem to balance the SE and EE for CRN with CSP is worth studying for wireless communication network.

# Bibliography

[1] A. Khattab, D. Perkins, and M. Bayoumi, “Cognitive radio networks: From theory to practice,” Springer Science and Business Media, 2012.

[2] I. F. Akyildiz, W. Y. Lee, M. C. Vuran, and S. Mohanty, “Next generation/dynamic spectrum access/cognitive radio wireless networks: A survey,” Computer Networks, vol. 50, no. 13, pp. 2127-2159, 2006.

[3] J. Mitola, and G. Q. Maguire, “Cognitive radio: Making software radios more personal,” IEEE Personal Communications, vol. 6, no. 4, pp.13-18. 1999.

[4] M. Masonta, M. Mzyece, and N. Ntlatlapa, “Spectrum decision in cognitive radio networks: A survey,” IEEE Communications Surveys and Tutorials, vol. 15, no. 3, pp. 1088-1107, 2013.

[5] H. Hu, H. Zhang, and Y. C. Liang, “On the spectrum- and energy efficiency tradeoff in cognitive radio networks,” IEEE Transactions on Communications, vol. 64, no. 2, pp. 490-501, Feb. 2016.

[6] I. F. Akyildiz, B. F. Lo, and R. Balakrishnan, “Cooperative spectrum sensing in cognitive radio networks: A survey,” Physical Communication, vol. 4, no. 1, pp. 40-62, 2011.

[7] T. Yucek and H. Arslan, “A survey of spectrum sensing algorithms for cognitive radio applications,” IEEE Communications Surveys and Tutorials, vol. 11, no. 1, pp. 116-130, 2009.

[8] X. Xing, T. Jing, W. Cheng, Y. Huo, and X. Cheng, “Spectrum prediction in cognitive radio networks,” IEEE Wireless Communications, vol. 20, no. 2, pp. 90-96, Apr. 2013.

[9] H. Eltom, S. Kandeepan, Y. C. Liang, B. Moran, and R. J. Evans, “HMM based cooperative spectrum occupancy prediction using hard fusion,” In Proc. IEEE International Conference on Communications, pp. 669-675, May. 2016.

[10] X. Xing, T. Jing, W. Cheng, Y. Huo, X. Cheng, and T. Znati, “Cooperative spectrum prediction in multi-PU multi-SU cognitive radio networks,” Mobile Networks and Applications, vol. 19, no. 4, pp. 502-511, Aug. 2014.

[11] S.D. Barnes, B.T. Maharaj, and A.S. Alfa, “Cooperative prediction for cognitive radio networks,” Wireless Personal Communications, vol. 89, no. 4, pp. 1177-1202, Aug. 2016.

[12] Y. Saleem and M. H. Rehmani, “Primary radio user activity models for cognitive radio networks: A survey,” Journal of Network and Computer Applications, vol. 43, pp. 1-16, Aug. 2014.

[13] V. K. Tumuluru, P. Wang, and D. Niyato, “Channel status prediction for cognitive radio networks,” Wireless Communications and Mobile Computing, vol. 12, no. 10, pp. 862-874, Jul. 2012.

[14] L. R. Rabiner, “A tutorial on hidden Markov models and selected applications in speech recognition,” Proceedings of the IEEE. vol. 77, no. 2, pp. 257-286, Feb. 1989.

[15] E. Tragos, S. Zeadally, A. Fragkiadakis, and V. Siris, “Spectrum assignment in cognitive radio networks: A comprehensive survey,” IEEE Communications Surveys and Tutorials, vol. 15, no. 3, pp. 1108-1135, 2013.

[16] E. Chatziantoniou, B. Allen, and V. Velisavljevic, "An HMM-based spectrum occupancy predictor for energy efficient cognitive radio," In Proc. IEEE International Symposium on Personal Indoor and Mobile Radio Communications, pp. 601-605, Sep. 2013.

[17] J. Yang, H. S. Zhao, X. Chen, J. Y. Xu, and J. Z. Zhang, "Energy-efficient design of spectrum prediction in cognitive radio networks: Prediction strategy and communication environment," In Proc. IEEE International Conference on Signal Processing, pp. 154-158, Oct. 2014.

[18] J. Yang and H. Zhao, "Enhanced throughput of cognitive radio networks by imperfect spectrum prediction," IEEE Communications Letters, vol. 19, no. 10, pp. 1738-1741, Oct. 2015.

[19] A. Bhowmick, K. Yadav, S. D. Roy and S. Kundu, "Throughput of an energy harvesting cognitive radio network based on prediction of primary user," IEEE Transactions on Vehicular Technology, Apr. 2017 (to appear).

[20] P. Thakur, A. Kumar, S. Pandit, G. Singh, and S. N. Satashia, "Performance analysis of high-traffic cognitive radio communication system using hybrid spectrum access, prediction and monitoring techniques, " Wireless Networks, 2017 (to appear).

[21] S. Xie, Y. Liu, Y. Zhang, and R. Yu, "A parallel cooperative spectrum sensing in cognitive radio networks," IEEE Transactions on Vehicular Technology, vol. 59, no. 8, pp. 4079-4092, Oct. 2010.